Lithium in Jack Hills zircons: Evidence for extensive weathering of Earth's earliest crust

Takayuki Ushikubo [a,*], Noriko T. Kita [a], Aaron J. Cavosie [b], Simon A. Wilde [c], Roberta L. Rudnick [d], John W. Valley [a]

[a] Department of Geology and Geophysics, University of Wisconsin, 1215 W. Dayton St., Madison, WI 53706, USA
[b] Department of Geology, University of Puerto Rico, PO Box 9017, Mayagüez Puerto Rico, 00681, USA
[c] Department of Applied Geology, Curtin University of Technology, Perth, WA 6102, Australia
[d] Geochemistry Laboratory, Department of Geology, University of Maryland, College Park, MD 20742, USA

ARTICLE INFO

ABSTRACT

In situ Li analyses of 4348 to 3362 Ma detrital zircons from the Jack Hills, Western Australia by SIMS reveal that the Li abundances (typically 10 to 60 ppm) are commonly over 10,000 times higher than in zircons crystallized from mantle-derived magmas and in mantle-derived zircon megacrysts (typically <2 ppb). High Li concentrations in zircons (10 to 250 ppm) have also been found in igneous zircons from three continental parent rocks: granites, Li-rich pegmatites, and migmatites in pelitic metasediment. The substitution of trivalent cations (REEs and Y) in zircon correlates with Li^{+1} and P^{+5}, suggesting that an interstitial site for Li, as well as the xenotime substitution for P, provides charge balance for REEs. Li is thus fixed in the zircon structure by coupled substitutions, and diffusive changes in [Li] composition are rate-limited by slow diffusion of REEs. The Jack Hills zircons also have fractionated lithium isotope ratios ($\delta^7Li = -19$ to $+13‰$) about five times more variable than those recorded in primitive ocean floor basalts (2 to 8‰), but similar to continental crust and its weathering products. Values of δ^7Li below $-10‰$ are found in zircons that formed as early as 4300 Ma. The high Li compositions indicate that primitive magmas were not the source of Jack Hills zircons and the fractionated values of δ^7Li suggest that highly weathered regolith was sampled by these early Archean magmas. These new Li data provide evidence that the parent magmas of ancient zircons from Jack Hills incorporated materials from the surface of the Earth that interacted at low temperature with liquid water. These data support the hypothesis that continental-type crust and oceans existed by 4300 Ma, within 250 million years of the formation of Earth and the low values of δ^7Li suggest that weathering was extensive in the early Archean.

1. Introduction

Recent evidence of moderately elevated $\delta^{18}O$ values in >4000 Ma zircons from the Jack Hills, Western Australia suggests that some of these grains grew in magma derived from hydrated crustal rocks, leading to the hypothesis that by 4200 Ma, the Earth had cooled sufficiently to allow the formation of proto-continental crust and oceans (Cavosie et al., 2007). In order to test these hypotheses, we have measured lithium content and isotope ratio in Jack Hills zircons. Previous studies have shown that Li isotopes are not significantly fractionated by igneous differentiation at high temperature (>800 °C) (Bryant et al., 2004; Teng et al., 2004, 2006a; Tomascak et al., 1999) while diffusive, hydrothermal, and weathering processes can fractionate δ^7Li with cumulative effects over 30‰ (Chan et al., 1992; Kisakürek et al., 2004; Rudnick et al., 2004; Teng et al., 2006b; Tomascak, 2004; Wunder et al., 2006). Thus the δ^7Li value in zircons can provide a tracer for processes of aqueous alteration and weathering at the Earth's surface, and the incorporation of surface-derived materials into crustal magmas. In this study, we report Li abundance (ppm) and Li isotope ratio (δ^7Li) for detrital zircons from Jack Hills, Western Australia that have U–Pb crystallization ages of 4348 to 3362 Ma. For comparison, we report analyses of a selected group of younger zircons. Because detrital zircons from Western Australia are the only known samples from the earliest Earth and the Jack Hills zircons are the best studied members of this suite, analysis of Li in these grains can provide unique chemical evidence of conditions during the first 500 million years of Earth history.

2. Samples

We measured the Li abundance and Li isotope ratios of 55 detrital zircons separated from Jack Hills metaconglomerate samples 01JH13 and 01JH54 (Cavosie 2005; Cavosie et al., 2004). Zircons were cast in epoxy and polished to their midsections. Most of the analyzed zircons had already been analyzed for U–Pb age, trace element chemistry, and oxygen isotope ratio (Cavosie 2005; Cavosie et al., 2004, 2005a, 2006).

For comparison, Li compositions were measured for zircons from primitive, mantle-derived rocks, ocean floor gabbro drilled along the Mid-Atlantic Ridge (Ocean Drilling Program, Leg 153, site 922) (Cavosie et al., 2005b) and kimberlite (KIM-5 zircon megacryst, Page et al., 2007a,b). Zircons were also studied from a range of settings in continental crust: migmatite in metasediment (P. J. Lancaster, personal communication); Middledale gabbroic diorite (Temora-1 and -2, Black et al., 2003, 2004); felsic pegmatite intrusion in wollastonite skarn (05ADK-2, Clechenko and Valley, 2003); zircon standard 91500 (Wiedenbeck et al., 2004); zircon standard Xinjiang (NMNH #146260); and zircons from four Li-rich granitic pegmatites. To evaluate the effect of metamorphism on Li in zircons, we measured δ^7Li and Li concentration of two zircons recovered from amphibolite facies (MH-02-10B-46, Rt. 812) and granulite facies (BMH-01-14-14, Treadway Mt.) migmatites from the Adirondack Mountains, NY. These zircons have detrital igneous cores that formed prior to metamorphism and overgrowths that formed during metamorphism. The U–Pb ages and O isotope ratios of these two zircons have been measured previously (Heumann et al., 2006; M. E. Bickford and P. J. Lancaster, personal communication).

3. Analytical methods

3.1. Standards for Li analysis by ion microprobe

Because ion microprobe analyses always show a matrix dependent bias for both isotope ratios and concentration, we established a new zircon standard for Li. This required examination of several samples. We made zircon grain mounts with 10–20 grains of each sample and investigated the homogeneity of Li isotope ratios and concentration by ion microprobe in order to choose the best zircon in terms of high Li abundance, and homogeneous isotope ratios and concentrations. As a result, we chose Xinjiang zircon to be used as the Li isotope standard (NMNH #146260), which came from a 20 g aggregate of 1–7 mm pale red crystals. Two aliquots (~40 and 18 mg) of Xinjiang zircon were dissolved in a mixture of HF and HNO_3 in high pressure Teflon bombs. Three separate cation exchange column purifications were performed on these dissolved stock solutions: two separations for the first dissolution and one for the second. Column chemistry followed the procedure outlined by Rudnick et al. (2004). Each of the purified Li solutions was analyzed multiple times by MC-ICP-MS at the University of Maryland yielding δ^7Li = 7.9±2.1‰ (2SD, 2SE = ±1.1‰), [Li] = 6.4±1.9 ppm (2SD, 2SE = ±1.1 ppm) (Table S1 in the Supplementary Information). We also used NIST-612 glass standard with known Li concentrations and isotope ratios (δ^7Li = 31.2‰, [Li] = 41.5 ppm, (Kasemann et al., 2005; Pearce et al., 1996)) as running standard to evaluate drift.

3.2. Li isotopic ratio and Li abundance

In situ analysis of Li isotope ratios and imaging of Li abundance were performed with a CAMECA IMS-1280 ion microprobe at the University of Wisconsin-Madison. The primary O^- beam was accelerated by 23 keV (−13 kV at ion source and −10 kV at sample) and shaped to 10 to 15 μm diameter at the sample surface in Kohler illumination mode with ion currents of 0.5 to 3 nA. Secondary ions were accelerated at +10 keV. Detailed secondary ion optics parameters include: entrance slit width of 120 μm, transfer lens setting of ×200 magnification, field aperture of 3000 μm square, and energy slit width of 40 eV. Li ions created at the edge of the sputtered pits are removed by collimating the secondary ion beam with the field aperture in order to reduce surface Li contamination. Under these conditions, transmission of secondary ions from the center of the pit is more than 70%. Lithium secondary ions ($^6Li^+$ and $^7Li^+$) were detected simultaneously by two small Hamamatsu electron multipliers at the extreme positions of the multicollection system (L2 and H2). The widest exit slits (500 μm), corresponding to mass resolving power of 2200, were sufficient to eliminate the interference of $^6Li^+$ on $^7Li^+$. Typical

secondary ion intensities of $^7Li^+$ were ~7×10^4 cps for NIST-612 glass and ~3×10^4 cps for Xinjiang zircon standard at primary ion currents of 1.5 nA and 2 nA, respectively. In each analytical session, we adjusted pulse height distribution to peak at 280 mV by adjusting the high voltages of individual EM detectors using Li isotope signals. In these conditions, EM yield is normally better than 99% compared to FC detectors and does not cause a significant discrimination on the measured ratios. Deadtime of each EM was ~70 ns, calibrated by measuring Si isotope ratios. We do not see any systematic changes in measured Li isotope ratios of NIST-612 glass with secondary Li ion currents by changing primary beam intensities. We used a Nuclear Magnetic Resonance (NMR) probe to regulate magnetic field, which provides a stable magnetic field ($\Delta M/M < 10$ ppm) for 10 h.

At each analysis position, we manually adjusted stage height (Z-focus) and applied automatic centering of the secondary ions before the isotopic measurement. Single analyses take ~12 min, consisting of 240 s for presputtering, ~60 s for secondary beam centering, and 400 s for collecting Li isotope signals (10 s × 40 cycles). In order to avoid aging of EMs, which may cause drift of EM gain and measured isotope ratios, we kept secondary ^7Li intensity lower than 7×10^4 cps. In this condition, repeated analyses of δ^7Li in NIST-612 glass standard did not drift more than 4‰ in 10 h of analysis.

The value of δ^7Li of sample zircons relative to the international Li standard, NIST SRM-8545 (LSVEC) and instrumental mass fractionation of the ion microprobe were calculated based on Li composition of the standard Xinjiang zircon (δ^7Li = 7.9‰; Table S1 in the Supplementary Information). The δ^7Li values of sample zircons were calculated as follows: The measured isotope ratios, $R_m = ^7Li/^6Li$, were divided by the literature value of LSVEC ($R_0 = ^7Li/^6Li = 12.039$; Chan et al., 1992). Instrumental mass fractionation (IMF) is defined as $\alpha = R_m/(R_0 * 1.0079)$ from standard Xinjiang zircon data.

Typically, 10 analyses of sample zircons were bracketed by a total of 6 to 8 analyses of the running standard and data were corrected for IMF based on α of bracketing standards. We used Xinjiang zircon as a running standard in the first (Jan. 10–12, 2007) and second sessions (Mar. 5–7, 2007), and later used NIST-612 glass as a running standard in the third session (May 21–23, 2007) (Table S4 in the Supplementary Information). The reproducibility of δ^7Li_m (= $[(R_m/R_0) - 1] \times 1000$) for Xinjiang zircon (typically ~±3‰, 2SD) is slightly larger than both that of NIST-612 (~±2‰, 2SD) and the internal error (~±2.0‰, 2SD), which may suggest minor δ^7Li heterogeneity in Xinjiang zircon. The IMF of glass (α_G) and zircon (α_Z) standards varied from 1.0306 to 1.0356 and 1.0234 to 1.0388, respectively, in three sessions though relative IMF between glass and Xinjiang zircon ($\alpha^* = \alpha_Z/\alpha_G$) calibrated in the same analytical sessions are nearly constant ($\alpha^* = 0.9997$, 1.0040, and 1.0028 for sessions 1, 2, and 3 within analytical uncertainty among different sessions). Thus, δ^7Li is calculated as $\delta^7Li = [(1 + \delta^7Li_m/1000)/a_Z - 1] \times 1000$ in the first and second sessions, and $\delta^7Li = [(1 + \delta^7Li_m/1000)/(a_G \times a^*) - 1] \times 1000$ in the third session. We report the larger value of either the internal error or spot-to-spot reproducibility of δ^7Li_m of running standards as measurement uncertainty. There could be small systematic bias of the IMF correction according to uncertainties of bulk analysis by ICP-MS (±2.1‰, 2 SD) and that of grain to grain heterogeneity (±1.1‰, 2 SE of average of 20 grains analyses by SIMS) in δ^7Li of Xinjiang zircon, however the potential effect of these factors would be to shift all of the ion microprobe data by a small constant factor. This would not affect the large fractionation of Li isotopes that is observed in our data.

Li concentration in zircon is estimated from the ratio of ^7Li count rate (I_{Li}, cps) to the primary beam intensity (Ip, nA), calibrating against Xinjiang zircon. We applied the $^7Li^+$ ion yield of zircon as 2550 (cps/nA/ppm (20 grains)) although the uncertainty of this value (±38%, 2SE) is worse than the reproducibility of the ion yield of homogeneous glass standard (±2.9%, 2SD) because the Li content in the Xinjiang zircon is heterogeneous.

After Li analysis, we imaged the bottoms of all ion microprobe pits by scanning electron microscope. We rejected data from irregular pits

Table 1
Values of δ^7Li, Li abundance, and U–Pb age of detrital zircons from the Jack Hills, Western Australia

Sample and spot #	δ^7Li	2σ[a]	Li (ppm)	Age (Ma)
01JH13a 2.5NM				
2-2.1	−10.6	±2.2	14.2	4030
3-1.1	−8.5	±2.2	39.4	3961
3-6.1	5.7	±2.2	31.3	4006
4-4.1	6.4	±2.2	16.7	4041
5-3.1	−3.8	±2.2	14.5	4073
6-2.1	6.4	±2.2	17.5	4040
6-3.1	2.0	±2.4	8.7	4136
9-1.1	7.2	±3.0	37.7	3577
01JH13a 2.5M				
1-3.1	−6.0	±3.0	18.8	4126
2-1.1	−1.7	±3.0	33.9	4016
3-3.1	−5.4	±3.5	2.6	4104
3-4.1	5.4	±3.0	30.9	4044
5-5.1	1.0	±3.0	38.6	4021
01JH13b 2.5NM				
7-2.1[b]	6.2	±1.9	33.1	3625
8-1.1[b]	−7.9	±1.9	33.6	4133
11-1.1	0.7	±3.0	6.0	4098
11-1.2	3.7	±3.0	8.1	4098
11-1.3	−0.7	±3.0	13.3	4098[c]
11-1.4	3.7	±3.0	11.9	4098[c]
11-1.5	−3.4	±3.0	15.7	4098[c]
19-1.1	2.1	±3.0	15.1	4066
19-1.2	−4.3	±3.0	12.9	4066[c]
19-1.3	6.1	±3.0	12.9	4066[c]
19-1.4	−0.3	±3.0	8.4	4066[c]
19-1.5[b]	−6.9	±6.9	1.2	4066
19-1.6[b]	−7.8	±3.0	4.6	4066
19-1.7[b]	−0.5	±3.0	10.0	4066[c]
19-1.8[b]	1.7	±2.8	9.2	4066[c]
19-1.9[b]	−0.1	±3.1	8.0	4066[c]
19-1.10[b]	−0.1	±1.9	23.2	4066[c]
20-2.1	−1.5	±3.7	6.5	3875
24-4.1	−9.5	±3.7	12.4	3846
25-8.1	13.4	±3.7	15.5	3821
01JH13b 2.5M				
1-3.1	−1.7	±3.3	11.7	4069[c]
2-1.1	−11.8	±3.3	8.8	4125
5-2.1	−1.8	±3.3	8.9	4017
6-3.1	1.4	±3.3	33.1	4089
8-4.1	−18.4	±3.3	48.8	4007
8-4.2[a]	−9.9	±2.0	51.9	4007
8-4.c1[b,d]	*−5.6*	*±2.1*	*26.0*	
8-4.3[b]	−10.5	±2.0	70.7	>4007[e]
10-4.1	−3.5	±3.3	10.1	3752
13-2.1	2.3	±3.3	23.8	4081
16-1.1	−10.1	±3.3	21.2	4054
18-1.1	−3.8	±2.2	11.0	4116
19-3.1	−5.1	±2.2	18.0	4187
24-1.1	−9.7	±2.2	49.0	4299
25-3.1	−0.9	±2.2	15.7	4154
01JH13b 5M				
2-1.1	−10.2	±5.0	1.3	4266
2-1.2[b]	−8.6	±3.3	9.3	4266
4-2.1	−16.7	±2.2	41.9	3589
4-2.2[b]	−6.6	±2.8	37.8	3589
4-2.3[b]	−12.1	±2.8	25.3	3904
6-2.c1[d]	*−7.2*	*±2.5*	*21.3*	
6-2.1	−0.3	±3.7	18.5	4229
10-2.1	−8.5	±2.5	13.5	4265
10-4.1	−4.7	±2.5	14.1	3631
12-4.1	−8.8	±2.5	10.9	(4081)[f]
14-1.1	−13.5	±2.5	31.4	4068
14-4.1	−0.6	±2.5	26.6	4033
14-4.2[b]	−8.3	±2.8	64.9	4033
20-1.1	−7.9	±2.5	14.9	4133
22-1.1[b]	−15.9	±2.8	31.6	4113
22-1.2[b]	−18.1	±2.8	26.9	4113
22-1.3[b]	−3.4	±2.8	25.7	4002
22-1.4[b]	−2.5	±2.8	25.0	>4113[e]
22-1.c1[b,d]	*1.2*	*±2.8*	*25.4*	
22-1.5[b]	−10.0	±2.8	47.0	4113[c]

Table 1 (*continued*)

Sample and spot #	δ^7Li	2σ[a]	Li (ppm)	Age (Ma)
01JH13b 5M				
22-1.6[b]	−7.5	±2.0	23.8	>4113[e]
22-1.c2[b,d]	*−8.1*	*±2.0*	*19.1*	
22-1.7[b]	−6.4	±2.2	21.1	>4113[e]
22-1.c3[b,d]	*−11.2*	*±2.0*	*34.1*	
22-2.1	−19.5	±2.5	25.8	(4128)[f]
22-2.2[b]	−2.4	±2.8	38.9	>4128[e]
22-4.1[b]	−0.9	±8.4	1.6	3743
01JH54a 2.5NM				
17.1	6.5	±3.1	41.2	4178
34.1	11.8	±3.1	39.5	4165
01JH54a 2.5M				
58.1[b]	3.6	±1.9	30.3	4063
58.2[b]	6.9	±2.2	20.7	4036
01JH54a 5M				
66.1	−4.0	±3.1	32.3	4195
68.1	−4.5	±3.1	44.3	4159
77.1	−11.8	±3.4	4.6	4282
78.1	4.5	±3.1	35.3	4167
78.2	1.5	±3.1	15.1	3362
81.1[b]	7.6	±1.7	30.1	4098
81.2[b]	8.1	±1.8	20.7	4103
81.3[b]	−1.6	±1.5	45.1	3649
01JH54a 10M				
90.1	0.7	±3.1	28.3	4263
90.2[b]	−0.6	±1.7	27.6	4030
D7.1	1.7	±3.1	36.3	4348
01JH54TS-001 thin section				
11.1	−1.2	±3.7	36.6	
11.2	−1.1	±3.7	37.3	
11.3	−3.6	±3.7	33.4	
11.4	−2.7	±3.7	27.0	
Quartz in 01JH54 Quartzite[g]				
Pebble (*n*=1)	5.8		0.4	
Matrix (*n*=1)	5.8		0.1	

[a] Errors are the larger values of either the internal error or reproducibility of standard analysis.
[b] NIST SRM 612 glass was used as a running standard. In other measurements, Xinjiang zircon was used as a running standard.
[c] The U–Pb age of core of zircon (see Fig. S2 in Supplementary Information).
[d] Li measurement pits on cracks shown in Fig. 1.
[e] The U–Pb age of different domain (see Fig. S2 in Supplementary Information).
[f] The U–Pb age of a different but close CL domain of the same zircon.
[g] measured by ICP-MS.

(e.g. pits containing cracks, inclusions, or overlapping the grain edge, see Cavosie et al., 2005a) although the results do not change if data from irregular pits are included. Rejected data are shown in Fig. S2 and Table S4 in the Supplementary Information.

3.3. Li ion imaging

Secondary ion images were obtained for construction of Li concentration maps on selected zircon grains. Before each scanning analysis, the sample was pre-sputtered over a 70 μm × 70 μm area by rastering a stronger primary beam (~10 μm in diameter, 2 nA) for 1000 s in order to eliminate surface contamination. Since the lateral resolution of an ion image is limited by the size of the primary beam, we used a focused beam of O^- with a diameter of 2 μm (~10 pA) to scan a 50 μm × 50 μm area. Each image was collected as 256 × 256 pixels (~0.2 μm/pixel). The Dynamic Transfer Optical System was applied to obtain a wide field of view and $^7Li^+$ was detected by the axial ETP electron multiplier. Other mass spectrometric conditions were similar to those used for isotopic analyses of the samples.

4. Results

Results of Li measurements for Jack Hills zircons are summarized in Table 1. Further data for Jack Hills zircons and those for other zircons forming part of this study are summarized in Tables S2 and S3,
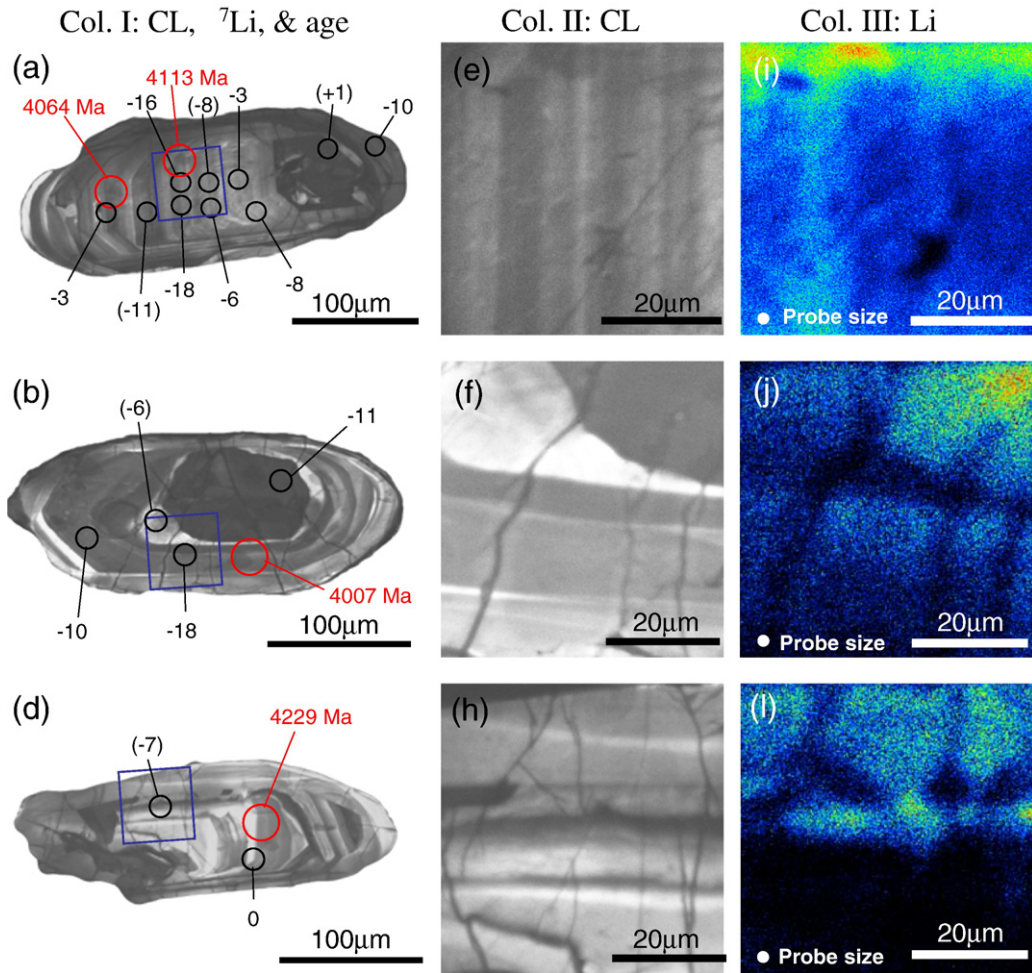
Fig. 1. Matching images showing the correlation of cathodoluminescence (CL) growth zoning, δ^7Li, and Li concentration for Jack Hills sample 01JH13b. Zircon numbers are: **(a)** 5 M 22-1, **(b)** 2.5 M 8-4, and **(c)** 5 M 6–2. CL images in Column I show magmatic growth zoning, ion microprobe pits, δ^7Li values, and concordant U–Pb ages. Parenthetic numbers are δ^7Li values of measurements made on cracks in zircon. Typical analytical uncertainty of δ^7Li is ~3‰ (2 SD). Squares indicate the field of view of enlarged images in the right-hand columns: CL in Column II and Li concentration in Column III (bright colors=higher [Li]). The smaller primary ion beam spot size (~2 μm) used for imaging is shown as a white spot (Col. III). Results of multiple analyses of δ^7Li and Li imaging of zircon grains indicate that individual CL domains have different δ^7Li and Li concentration. The apparent width of Li-poor open cracks in Column III is broadened with respect to that in CL images by analytical effects (see text).

respectively, in the Supplementary Information, along with U–Pb ages and oxygen isotope ratios that were previously reported (Cavosie, 2005; Cavosie et al., 2004, 2005a, 2006; unpublished data). Detailed results of the three sessions for Li analyses of Jack Hills zircons, and CL images showing the analyzed positions, are presented in Table S4 and Fig. S2 in the Supplementary Information. In most cases, we made one Li isotope analysis per zircon, however, we made multiple Li isotopic analyses and more Li imaging on selected zircons where appropriate.

Fig. 1 shows matching images for three Jack Hills zircons whose U–Pb ages are older than 4000 Ma (Table 2). For each zircon, multiple Li isotope analyses, Li images, and CL images are correlated. We did not find any Li hot spots in the Li images nor spikes of Li ion signal during Li isotope analyses, that would suggest the existence of Li enriched inclusions. These results imply that Li is hosted in zircon and homogeneously distributed within single growth zones of the zircons. The combination of *in situ* analysis and CL imaging allows data to be correlated with the U–Pb age and δ^{18}O for specific domains within each zircon. Importantly, Jack Hills zircons are zoned in both δ^7Li and Li concentration and these values correlate with igneous growth zoning (e.g. Fig. 1a).

The Li images in Fig. 1 show crosscutting dark zones that clearly correspond to cracks seen by CL. The dark zones in Li content maps

appear wider than cracks in CL because of the larger beam size and the shallower depth of field of the ion microprobe as compared to the SEM. Detailed traverses of these cracks by Zygo™ white light interferometer measures their relief at the nm-scale. Typically, the

Table 2
Compositions of Li, REEs, Y, and P in Jack Hills zircons

Sample	Li spot #[a]	REE spot #[b]	Li (ppm)	ΣREE[b] (ppm)	Y[b] (ppm)	P[b] (ppm)	$(Y+REE)/P$ (atomic)[b]	$(Y+REE)/(Li+P)$ (atomic)
01JH54a-17	1	1	44	715	821	240	1.74	0.96
01JH54a-34	1	1	42	519	538	158	1.79	0.82
01JH54a-58	1	2	32	911	1081	411	1.33	0.99
	2	1	22	588	692	263	1.33	0.97
01JH54a-77	1	7	7	1416	1774	692	1.27	1.22
01JH54a-81	1	2	32	1624	1838	326	2.87	2.00
	2	4	22	1544	1859	295	3.16	2.37
	3	3	48	159	144	83	0.96	0.27
01JH54a-90	2	2	29	2117	2316	996	1.21	1.07
D7	1	1	39	1216	1536	280	2.71	1.67
Average							1.84	1.23

[a] Spot positions are shown in Fig. S2 in the supplementary information.
[b] Data from Cavosie et al., 2006.

cracks form "V-shaped valleys" where they intersect the polished surface. The SEM image has good depth of field and sees to the bottom of the valleys, recording narrow cracks. The ion microprobe is focused on the polished surface and detection is less efficient along the sides of these valleys, making cracks appear wider than seen by SEM. Thus, the width of these dark cross-cutting zones in the Li images is an analytical artifact and should not be mistaken as evidence for Li-depleted zones adjacent to cracks.

Fig. 2 shows the relation between δ^7Li and U–Pb ages of Jack Hills zircons (Fig. 2a) and the relation between δ^7Li and Li abundance of the measured zircons (Fig. 2b). For comparison, Fig. 2b also shows igneous zircons from younger rocks from a variety of tectonic settings, including kimberlite, and oceanic and continental crust. Zircons from Li-rich pegmatites and metamorphic overgrowths on zircons from migmatites of metasedimentary origin are enriched in Li (typically >30 ppm). In contrast, zircons from kimberlite and oceanic crust gabbro have low Li contents (<8 ppb). It is not possible to precisely determine δ^7Li in these low [Li] samples by ion microprobe and thus they are plotted at 4‰ in Fig. 2b, the average value for mantle rocks. Other zircons from continental crust, including detrital igneous cores of zircons from the migmatites, contain moderate levels of Li (0.2 to ~20 ppm). The Jack Hills zircons are characterized by highly fractionated Li isotopes ($\delta^7Li = -19$ to +13‰) (Fig. 2a), and high Li

concentrations (1.2 to 71 ppm) (Fig. 2b). No correlation is observed between Li abundance, δ^7Li, age, or age concordance. However, it is of interest to note that low δ^7Li values are seen in zircons as old as 4300 Ma.

Multiple Li isotope analyses of two zircons recovered from migmatites from the Adirondack Mountains, NY are shown in Fig. 3, together with U–Pb ages and $\delta^{18}O$. It is evident that Li concentration of the detrital cores is low (1 to 2 ppm) compared with that of the metamorphic overgrowths (>20 ppm). However, no extremely low (<−10‰) or high (>10‰) δ^7Li values were observed in these zircons in spite of intense prolonged metamorphism at amphibolite facies (MH-02-10B-46) or granulite facies metamorphism (BMH-01-14-14) (Kitchen and Valley, 1995; McLelland et al., 2004; Valley et al., 1990).

5. Discussion

5.1. Li substitution in zircon

Fig. 4 summarizes Li concentration in zircons determined by ion microprobe in this study. While igneous zircons from primitive magmas generally contain less than 8 ppb Li (Fig. 4b), many zircons from evolved magmas in continental crust are abundant in Li (10 to 70 ppm) (Fig. 4c). One zircon from the Harding pegmatite contains
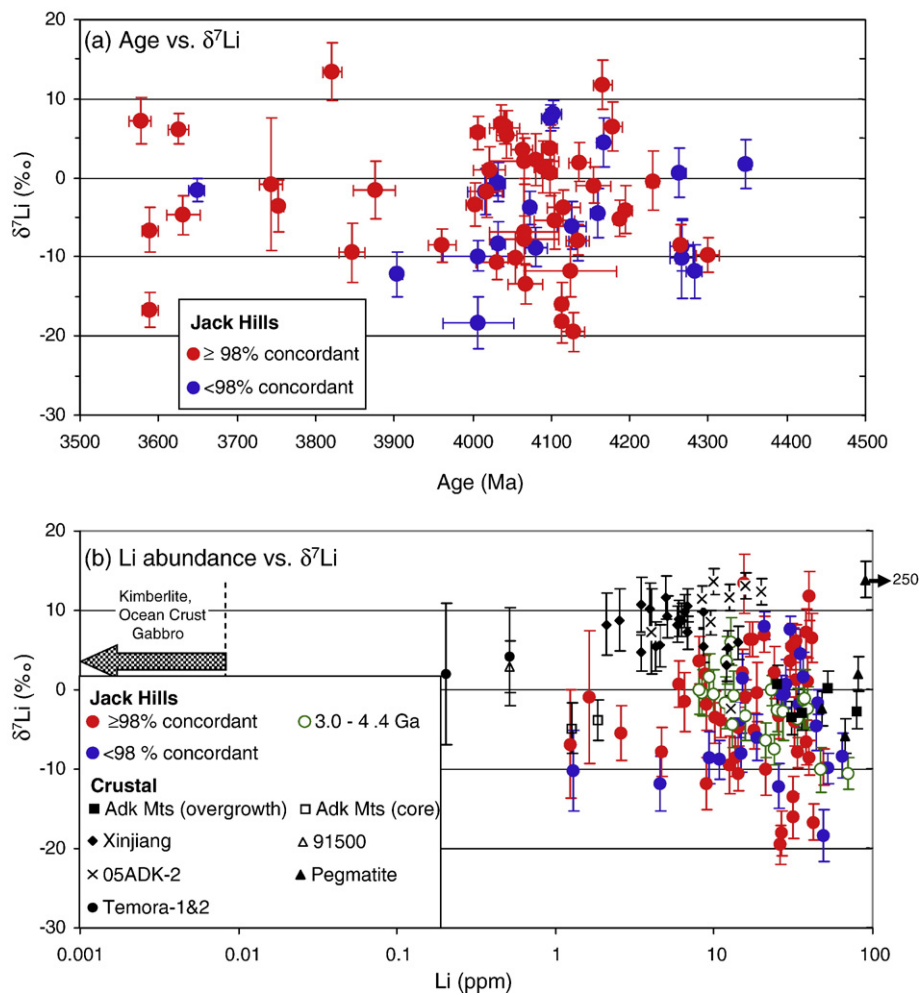

Fig. 2. (a) δ^7Li vs. U–Pb age for Jack Hills zircons. *In situ* analyses were located within specific CL domains. (b) δ^7Li vs. Li concentration (ppm) for Jack Hills detrital zircons and zircons from known protoliths, including continental crust (Table 1, and Table S2 and S3 in the Supplementary Information). Li abundances in zircons from kimberlite and ocean crust gabbro are too low (<0.05–8 ppb) for precise isotopic analysis and are plotted at average δ^7Li (WR). The dashed line at 0.008 ppm shows the upper limit of these Li abundances for primitive magmas. Analytical uncertainties for δ^7Li and age are 2SD. Symbols: red circles = Jack Hills zircons with ≥98% concordant U–Pb ages; blue circles = 85–97% concordant Jack Hills zircons; open circles = domains in Jack Hills zircon with no age data, smaller black symbols are selected zircons from younger continental crust (Table S3 in the Supplementary Information).
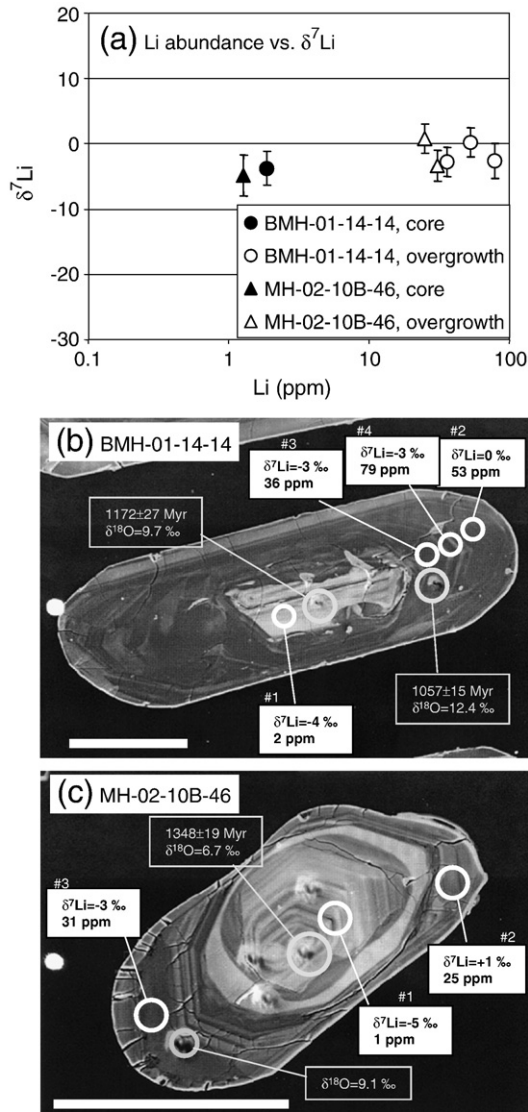
Fig. 3. Li and O isotope ratios, U–Pb age, and CL Images of Adirondack Mountains zircons. (a) δ^7Li vs. Li concentration (ppm) for Adirondack zircons. Uncertainty is at 2SD. CL Images of (b) BMH-01-14-14 from granulite facies migmatite at Treadway Mt., (c) MH-02-10B-46 from amphibolite facies migmatite at Rt. 812. Li and O isotope ratios, and U–Pb age are also shown. Scale bars are 100 μm.

250 ppm Li (Fig. 2b). These igneous zircons are surprisingly rich in Li and such compositions have not been widely recognized. High Li concentrations raise the question of what controls Li substitution in zircon. Possible factors include: Li-rich compositions of parent melts, the composition of other elements linked to Li by coupled substitutions, and the conditions of zircon crystallization.

High Li content has thus far been analyzed by an ion microprobe in zircons with known host rocks in two settings: Li-rich pegmatites that contain Li-bearing minerals (spodumene, lepidolite, triphylite, and elbaite) and migmatites that formed by anatexis of surrounding amphibolite- and granulite-facies metasediments. The highest measured Li concentration (250 ppm, Harding pegmatite) shows that natural zircons can contain several hundred ppm of Li.

Lithium ions have an appropriate size to substitute for Zr^{VIII} in the zircon structure. The ionic radius of Li^{+1} in eight-fold coordination with oxygen is 0.092 nm, which is slightly larger than Zr^{+4} (0.084 nm), but smaller than the REEs that also substitute for Zr^{VIII} (Shannon 1976). However, charge balance is also a constraint. Several coupled charge-balanced substitutions have been proposed for zircon (Finch et al.,

2001, Hanchar et al., 2001, Hoskin and Schaltegger, 2003) including the xenotime substitution

$$(Y, REE)^{3+} + P^{5+} = Zr^{4+} + Si^{4+} \tag{1}$$

and the interstitial substitution,

$$Li^{1+}_{(interstitial)} + (Y, REE)^{3+} = Zr^{4+} + \square \tag{2}$$

Thus, both the Li concentration in magma and the concentrations of other elements required for charge-balanced substitutions can play a role in determining the amount of Li in zircon, but experiments and mineral analysis are required to verify these predictions.

Many studies have analyzed trace elements in zircon including REEs, Y and P. Rather than finding that atoms of (Y+REEs)=P as would be predicted by Eq. (1), there commonly is an excess of trivalent cations and insufficient P for charge balance (Hoskin and Schaltegger 2003). In the Jack Hills zircons, the atomic ratio of (Y+REEs)/P ranges from 0.96 to 3.16 with an average of 1.84 (Cavosie et al., 2006).

Experiments show that zircons grown in Li–Mo flux can contain more than 100 ppm Li if REEs are present. In contrast, zircons grown in Li–Mo flux in the absence of REEs contain <1 ppm Li (Hanchar et al., 2001). This suggests that Li concentration in zircon is strongly linked to REE abundance in zircon by Eq. (2).

The Jack Hills zircons are the only sample suite for which the necessary trace elements have been measured to evaluate both substitutions (1) and (2). Table 2 summarizes Li, P, REE, and Y abundances, the ratio of (REE+Y)/P (substitution 1), and the ratio of
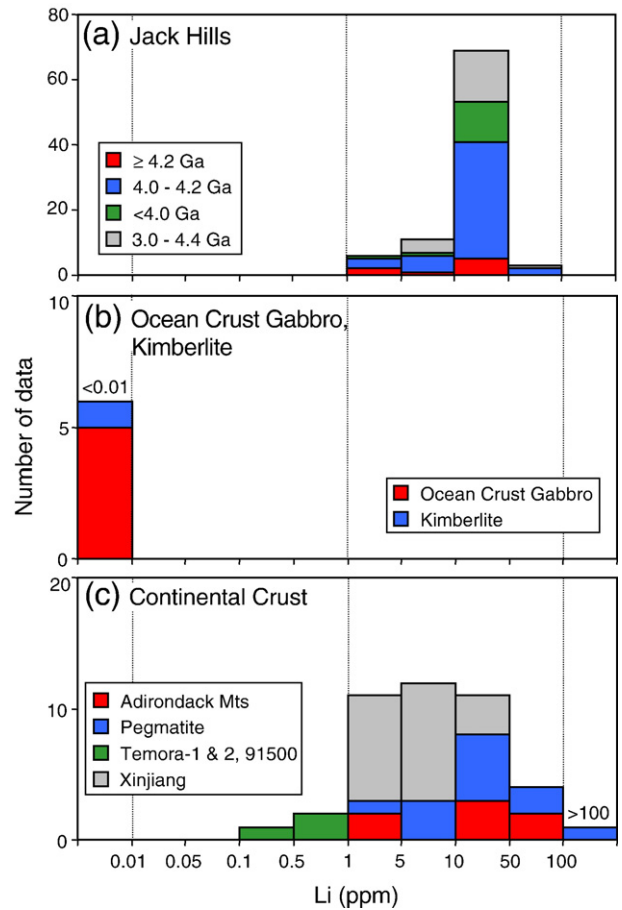

Fig. 4. Li abundance (ppm) of (a) Jack Hills zircons; (b) Ocean crust gabbro and Kimberlite zircons; (c) Continental crust zircons from Adirondack Mountains, pegmatites, Temora-1, Temora-2, 91500, and Xinjiang measured by an ion microprobe (Table 1, and Table S2 and S3 in the Supplementary Information).

(REE+Y)/(Li+P) (substitutions 1 and 2) (Cavosie et al., 2006; this study). These analyses are from multiple sessions by ion microprobe and the analysis pits were correlated to be within approximately the same growth zones of each zircon. It is likely that these correlations will be improved with more data and if all elements are analyzed from the same spot. Nevertheless, it is apparent that a combination of both substitutions (1) and (2) explains the mineral chemistry better than just the xenotime substitution (1). While the average value of (REE+Y)/P is 1.84, the ratio drops to (REE+Y)/(Li+P)=1.23 when Li is considered. These data strongly support the experiments that show Li substitution in the zircon structure by an interstitial mechanism. Thus, Li^{+1} provides the charge balance necessary for significant amounts of trivalent cations. In fact, because of its low atomic weight, Li is disproportionally important and 10 ppm Li is sufficient to balance over 200 ppm of REEs. In some zircons the presence of lithium may be more important than phosphorus for explaining the REE content.

5.2. Evaluation of variable Li compositions in the Jack Hills zircon suite

The use of Li in zircon to trace magmatic sources requires that primary Li composition and isotopic ratios remain preserved through subsolidus processes, and that Li diffusion in zircon is slow. It has been shown that Li isotopic fractionation can occur at magmatic temperatures due to chemical diffusion since the diffusion rate of ^6Li in grain boundary fluids and melts is faster than that of ^7Li (Jeffcoate et al., 2007; Lundstrom et al., 2005; Richter et al., 2003; Rudnick and Ionov, 2007; Teng et al., 2006b). It has also been shown that clinopyroxene and olivine can exchange Li by diffusion at high temperature (Coogan et al., 2005; Dohmen et al., 2007; Spandler and O'Neill, 2006), however, no data exist for the diffusion rate of Li in zircon.

The interstitial substitution for Li in zircon (Eq. (2)) would indicate that Li is linked to REEs and Y, and thus that changes in the Li concentration by chemical diffusion are rate-limited by the diffusion rate of these trivalent cations. Experiments and the common observation of growth zoning in igneous zircons show that diffusion of REEs is slow even at magmatic temperatures (Cherniak et al., 1997, Cherniak and Watson 2003). The immobilization of Li would preclude processes of isotope fractionation that are driven by chemical diffusion described above, but does not constrain the rates of Li isotope exchange by self diffusion in zircon. For this reason, we have empirically evaluated the effect of any sub-solidus diffusive exchange on Li composition in zircons based on zoning in natural zircons.

The patterns seen in scanning ion images of Li concentration correlate with those in CL images in all four Jack Hills zircons that were imaged and are older than 4000 Ma. Dark CL bands tend to be more Li-rich (Fig. 1). Dark CL bands also tend to be richer in REE, Th, and U (Cavosie et al., 2006).

The coincidence of lithium and CL zoning provides a test to evaluate potential sub-solidus alteration. If Li diffused slowly into zircons from the grain boundaries and exchange was arrested, then one would expect to see Li-rich rims and a progressive exchange in δ^7Li from values similar to the source of Li to low values due to faster ^6Li diffusion (Parkinson et al., 2007; Richter et al., 2003). In this case, the sharp oscillatory gradients, Li-poor rims, and δ^7Li patterns seen in Fig. 1 would be overprinted. Thus, if Li enrichment in Jack Hills detrital zircons had been caused simply by chemical diffusion after crystallization, it would be unreasonably fortuitous for the Li abundance to correlate with the pattern of concentric, oscillatory magmatic growth-zoning seen in CL images. In addition, the cores of zircons have either higher or lower Li abundance than their rims. Furthermore, as discussed above, neither Li enrichment nor depletion is observed adjacent to open cracks in maps of Li abundance (Fig. 1, Col. III). Li concentrations from ion microprobe pits on cracks do not show any significant difference from regular pits (Fig. S1 in the Supplementary Information). These results show that Li composition of Jack Hills zircons have not been modified by cracks that can be seen in

the samples today. Thus, there is no evidence that indicates the Li enrichment measured in Jack Hills zircons is caused by post-crystallization processes.

Zircons from the Adirondack Mountains, NY provide further evidence that zircons reliably preserve both their original Li concentration and isotopic composition. Mineral equilibria and *in situ* U–Pb geochronology of these zircons show that they were subjected to prolonged high-grade metamorphism (MH-02-10B-46, upper amphibolite facies, ~675 °C; BMH-01-14-14, granulite facies, ~750 °C), anatexis, and slow cooling of 1–2 °C/Myr (Heumann et al., 2006; Kitchen and Valley, 1995; McLelland et al., 2004; Valley et al., 1990). The igneous cores of these zircons are Li-poor even though their metamorphic overgrowths contain ~20 times higher Li abundances (Fig. 3). The low [Li] in igneous cores is consistent with that of many potential parent magmas. If Li enrichment of over-growths was caused by Li diffusion, then low δ^7Li values would be observed in overgrowths. However, this is not the case. Consistently higher Li concentrations in anatectic overgrowths are explained because Li-rich overgrowths crystallized from partial melts of metasediment, Li is mildly incompatible, and these pelitic migmatites formed from originally clay-rich sediments that were likely Li-rich. This explanation is consistent with the homogeneous oxygen isotope ratios within overgrowths and the steep gradients of $\delta^{18}O$ between igneous cores and metamorphic overgrowths of Adirondack zircons (Page et al., 2007a,b; Peck et al., 2003; P. J. Lancaster, personal communication). In this case, the detrital (igneous) cores of these zircons were xenocrysts in Li-rich partial melts from which the Li-rich overgrowths formed. Existence of Li-poor igneous cores indicates that primary igneous Li composition of igneous cores of zircons are preserved in ~1000 Ma migmatites that formed and cooled slowly from 750 °C even though the Li-poor cores were encased by Li-rich zircon overgrowths.

It could be hypothesized that the gradients in Li composition reflect slow exchange of Li in zircon that is linked to slow chemical diffusion of REEs, but that Li self diffusion might be faster. As discussed earlier, this possibility arises if the substitution of Li in zircon is by charge-balanced trivalent cations that diffuse slowly (e.g. Y, REE^{3+}) (Cherniak et al., 1997), in which case gradients in [Li] may reflect the sluggish exchange of REEs. However, we conclude that Li self diffusion is also slow and that diffusion did not affect Li isotope ratios in zircons in this study, based on the following observations:

1) Some zircons have variable δ^7Li but show no correlation between δ^7Li and distance from the grain edge. In contrast, single growth bands seen by CL are homogeneous in δ^7Li within spatial resolution (10 to 15 μm) and analytical precision (±2–3‰ 2SD; e.g., Fig. 1a). Thus, Li abundance and δ^7Li correlate within single igneous growth bands. This is not consistent with rapid self diffusion of Li from grain boundaries into zircons.

2) Most low δ^7Li values (<−10‰) are observed in Li-rich domains (9 to 71 ppm) (Fig. 2b). If the alternative interpretation, that Li self diffusion is faster than chemical diffusion was correct, then the low δ^7Li values of Jack Hills zircons would be caused by localized Li isotopic exchange between different igneous growth bands. However, this interpretation is not favored because low δ^7Li values would be observed in Li poor domains where even small amounts of Li exchange could change the Li isotope ratio—and this is not observed. Thus, intracrystalline exchange by Li self diffusion is also inconsistent with our results.

3) The Li-poor igneous cores from the Adirondack migmatite zircons do not have systematically lower δ^7Li than the overgrowths. As discussed above, these igneous zircon cores were preserved in migmatites that attained temperatures up to 750 °C. Lower δ^7Li would be expected if even small amounts of Li diffused into the cores from the Li-rich overgrowths (Fig. 3). The Adirondack zircons thus provide important direct evidence that Li diffusion in zircon is slow.

It could also be hypothesized that Li exchange has been facilitated by non-diffusive processes. However, we conclude that while recrystallization and radiation damage certainly occur in zircons, such disturbances can generally be recognized (and avoided) based on the following arguments.

1) The comparison of U–Pb ages to Li (ppm) and δ^7Li measured *in situ* by ion microprobe provides an additional test of reliability for the Li data. The good U–Pb concordance and agreement of ages among different crystals shows that these specific domains of single zircons have not recrystallized.

2) There is no significant difference between Li abundance and δ^7Li for zircons that show highly concordant (≥98%) U–Pb ages and others that are 85–97% concordant (Fig. 2, Table S2 in the Supplementary Information). This indicates that Pb loss, which caused the mildly discordant ages, did not significantly affect magmatic Li compositions in zircon.

Taken together, these results indicate that Jack Hills zircons were not enriched in Li by sub-solidus processes. These results further support the conclusion that δ^7Li values are primary monitors of original magmas.

The lack of post-crystallization Li exchange in Jack Hills zircons is partly the result of their occurrence in highly mature (>95% SiO$_2$) sedimentary host rocks (Cavosie et al., 2004). The Jack Hills detrital zircons were deposited in conglomerates and sandstones at ~3000 Ma, and metamorphosed to ~500 °C at 2600 Ma (Cavosie et al., 2007). Most zircons are surrounded by quartz that contains less than 0.4 ppm Li (Table 1). Thus metamorphic exchange with quartz over the past 3000 Ma can be further ruled out as a cause of the Li-rich compositions.

It has been proposed that Jack Hills zircons were overprinted by high-grade metamorphism or hydrothermal alteration before 4000 Ma (Hoskin, 2005; Nemchin et al., 2006). However, those studies describe distinctive zircons that differ from the domains analyzed in this investigation. Unlike those zircons, the zircons of this study preserve magmatic chemistry (age concordant) and internal structure (magmatic growth zoning) (Cavosie et al., 2006, 2007). Thus, our results strongly support the conclusion that the parent magmas of Jack Hills zircons had protoliths that were Li-rich and isotopically fractionated.

5.3. Low δ^7Li: evidence for weathering of the early Archean crust

In this study, we find wide variations in Li concentration in zircons of more than 6 orders of magnitude (<8 ppb to 250 ppm, Fig. 2b). The observed high Li concentrations in Jack Hills zircons, typically 10 to 60 ppm, are commonly over 10,000 times higher than in zircons from ocean crust gabbros (Fig. 4). In this respect, they are comparable to those of zircons from granitic pegmatites and pelitic migmatites suggesting that these >4000 Ma zircons crystallized in an evolved magma that assimilated surface material. Furthermore, the extremely low δ^7Li (<−10‰) observed in some Jack Hills zircons provide constraints on the origin of Jack Hills zircons.

In order to understand the significance of the Li isotopic compositions, we compare the δ^7Li of the Jack Hills zircon with whole rock δ^7Li values for younger rocks (Fig. 5). While zircon is highly retentive of Li composition, as discussed above, it has been shown that diffusive exchange of Li is faster in other minerals, which can lead to kinetic isotopic fractionation in phenocrysts (for some minerals) and mantle xenoliths (Beck et al., 2006; Halama et al., 2007; Jeffcoate et al., 2007; Parkinson et al., 2007; Rudnick and Ionov 2007). To eliminate any bias from such effects, we use whole rock δ^7Li data when analyses of zircon are not available. While there may be a small fractionation of δ^7Li between zircon and host magma, empirical studies of magmatic differentiation indicate that Li isotopic fractionation is limited at magmatic temperatures (Δ<5‰) (Bryant et al., 2004; Halama et al., 2007; Marks et al., 2007; Teng et al., 2004) and can be ignored in a first order examination of possible protoliths to Jack Hills zircons.
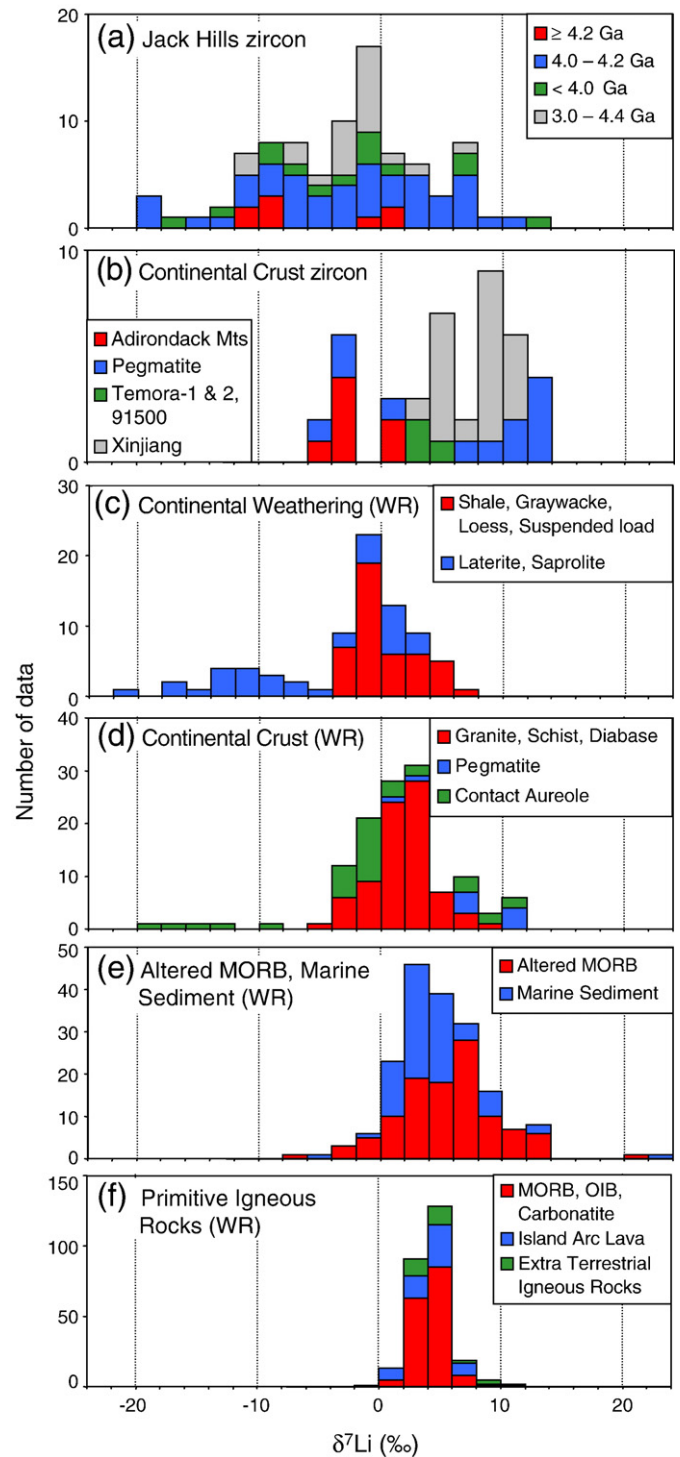

Fig. 5. Values of δ^7Li: (a) Jack Hills detrital zircons (this study); (b) Continental crust zircons (this study); and whole rock values for: (c) products of continental weathering; (d) continental crust; (e) altered ocean crust, marine sediment; (f) mid-ocean ridge basalt (MORB), oceanic island basalt (OIB), carbonatite, island arc lava, and extra-terrestrial igneous rocks (lunar rocks and regolith, Martian meteorites, eucrites, and silicates in pallasite and iron meteorite). References are listed as follows: (c) Huh et al., 2001; Kisakürek et al., 2004; Moriguti and Nakamura, 1998; Rudnick et al., 2004; Teng et al., 2004; (d) Bryant et al., 2004; Kisakürek et al., 2004; Rudnick et al., 2004; Teng et al., 2004, 2006a, 2006b, 2007; (e) Benton et al., 2004; Bouman et al., 2004; Chan and Frey, 2003; Chan et al., 1992, 2002a, 2006; Kobayashi et al., 2004; (f) Chan and Frey, 2003; Chan et al., 1992, 2002b; Elliot et al., 2006; Halama et al., 2007, 2008; Kobayashi et al., 2004; Magna et al., 2006a, 2006b; Moriguti and Nakamura, 1998; Nishio et al., 2007; Ryan and Kyle, 2004; Seitz et al., 2007; Tomascak et al., 2000, 2008.

Fig. 5 shows the range of δ^7Li values of Jack Hills zircons (Fig. 5a) and continental crust zircons in this study (Fig. 5b) compared to products of continental weathering (Fig. 5c), continental crust (Fig. 5d), altered ocean crust and marine sediments (Fig. 5e), primitive igneous terrestrial rocks (MORB (mid-ocean ridge basalt), OIB ocean island basalt), carbonatite, and island arc lava) and extra terrestrial igneous rocks (Lunar rocks and regolith, Martian meteorites, eucrites, and silicates in a pallasite and an iron meteorite) (Fig. 5f). Values of δ^7Li are relatively constant in primitive rocks derived from the Earth's mantle (MORB, OIB, and carbonatite; average 4.2 ± 2.6‰ 2SD) (Fig. 5f). Values from the Moon, Mars, and eucrites are also similar to the Earth's mantle (Fig. 5f). Altered ocean crust, including hydrated MORB, serpentinized peridotite (5.5 ± 8.1‰), and marine sediment (4.1 ± 7.3‰) are similar in average value, but more variable (Fig. 5e) because of interaction with sea water (δ^7Li$=\sim+32$‰ (Tomascak, 2004)). Values of δ^7Li are lowest and most variable in rocks from continental crust, including granites, schists, pegmatites, clays, and saprolites ($+11$ to -20‰; Figs. 5c and 5d). While the data set for δ^7Li below -10‰ is small, low δ^7Li correlates to higher values of CIA (chemical index of alteration) suggesting the importance of clay minerals (Rudnick et al., 2004).

The variability of δ^7Li in Jack Hills zircons, including some of the lowest values ever measured, is significantly different from that in primitive magmas derived from the mantle (Fig. 5). The highly fractionated values of δ^7Li found in Jack Hills zircons (Fig. 5a) match those of weathered or evolved components of continental crust (Fig. 5c). As noted above, the concentrations of Li in these zircons are commonly over 10,000 times higher than in zircons from mantle-derived melts. These differences show that the parent igneous rock to Jack Hills zircons was not fresh ocean crust. Further support for this conclusion has recently been provided by the use of U–Yb, U/Yb–Hf and U/Yb–Y plots that allow good discrimination between zircons grown in modern oceanic crust from those that evolved in continental granitoids. Importantly, the Jack Hills zircons plot in the continental granitoid field (Grimes et al., 2007).

Low values of δ^7Li have also been found adjacent to certain plutonic rocks in hydrothermal diffusion aureoles (Marks et al., 2007; Teng et al., 2006b). However this process is unlikely to explain the Jack Hills zircon data because: 1) it is a mixing process that creates Li concentrations intermediate between the protoliths and does not explain the high concentrations of Li found in Jack Hills zircons; 2) exchange is by advection and chemical diffusion; and 3) the amount of fractionated Li formed in this manner is small in comparison to that produced during continental weathering. Furthermore, kinetic fractionation in contact aureoles can only be preserved at the low temperatures and short time-scales that prevail in shallow crust, and thus if some of the δ^7Li values in the Jack Hills zircons reflect a component such as this it also points to a shallow crustal environment.

The fractionated and highly variable δ^7Li values of Jack Hills zircons are best explained as the result of aqueous alteration at the surface of the Earth, which created protolith material such as clay-rich sediment, sea floor altered basalt, or saprolite, in a manner akin to the processes proposed to cause mildly elevated oxygen isotope ratios in Jack Hills zircons (Cavosie et al., 2005a, 2006, 2007). These isotopically fractionated Li-rich protoliths were buried and eventually melted to form magmas in which the zircons grew.

The new Li in zircon data provide evidence to constrain the environment of aqueous alteration. The Li content and δ^7Li of the oceans are strongly influenced by terrestrial weathering and sea water alteration of ocean crust due to partitioning of Li (with elevated δ^7Li) into water relative to most minerals. Was this process dominated by sub-marine alteration or by sub-aerial weathering? There are two possibilities. 1) if there was little continental crust to weather on the early Earth or freeboard was small, then this would tend to make early Archean sea water lower in ppm Li and δ^7Li, and closer to the mantle value (δ^7Li ~ 4‰) (Elliot et al., 2006; Jeffcoate

et al., 2007; Magna et al., 2006b; Seitz et al., 2004) than modern sea water (~ 32‰). Lower δ^7Li sea water would decrease δ^7Li for marine sediments that could potentially be incorporated into parent magmas of Jack Hills zircon. Alternatively, 2) if the amounts of continental crust and freeboard were relatively high, then more sub-aerial weathering would have occurred, the oceans would be more like today, and the amount of low δ^7Li weathered regolith would be greater. If the second model is correct, it would suggest that low values of δ^7Li in Jack Hills zircon came from the Li-rich weathering products of continental crust.

It is currently unknown whether plate tectonic processes as currently operative were in place on the early Earth. However, although it is impossible to evaluate the effects of seafloor spreading before 4 Ga, we point out that there is no evidence for large changes of δ^7Li in mantle-derived magma over time (Halama et al., 2008). Thus, the main difference in possible pre-4 Ga ocean ridge systems would be that higher heat flow would cause higher temperatures and more vigorous alteration. The effect of higher temperature would be to reduce isotope fractionation and that would have less affect if alteration products were to contaminate magmas. In addition, thus far, no zircons have been located in modern ocean crust with either the elemental concentrations or isotope ratios of Jack Hills zircons and no hydrothermally altered crust has low values of δ^7Li. Therefore the available evidence supports the latter model and the existence of large exposed landmasses at ~ 4300 Ma.

Furthermore, sub-aerial weathering would have been intense on the early Earth, if the atmosphere was CO_2-rich (e.g., Kasting, 1993) and surface temperatures were above 50 °C. In this case, incorporation of regolith with low δ^7Li and high Li abundance into crustal melts would explain the isotopically light compositions recorded by some Jack Hills zircons.

One consequence of intense weathering on the early Earth would have been extensive destruction of surface rocks. This offers a solution to the enigma that the oldest recognizable rocks are ~ 4000 Ma old, whereas the Jack Hills zircons are up to 400 million years older. It has been assumed that the answer to this question lies in heavy bombardment or extensive melting, but the process may be more benign. Deep weathering and disaggregation of igneous rocks could leave quartz and other minerals that are difficult to date even if this material has been preserved on the surface of Earth. Only the zircons would be recognizable as ancient.

The Li compositions of early Archean igneous zircons support and extend previous conclusions based on mildly elevated values of δ^{18}O in Jack Hills zircons. Zircons older than 4300 Ma have high Li abundances (up to 49 ppm) with low δ^7Li (~-10‰) (Table 1). The observed δ^7Li variation and especially the low δ^7Li indicate that magmas and their protoliths had differentiated within the crust and reacted with water at shallow levels within 250 million years of the formation of the Earth. These light stable isotope ratios strongly support the existence of chemically differentiated crust and oceans that could have been hospitable to life at 4300 Ma and possibly earlier.

6. Conclusions

Li abundance and Li isotope ratios of 4348 to 3362 Ma detrital zircons from the Jack Hills, Western Australia, were measured by SIMS and we found that the Jack Hills zircons have high Li concentration (typically 10 to 60 ppm) and large fractionation in the δ^7Li value (-19 to $+13$‰). These values distinctly differ from those of zircons from primitive, mantle-derived magmas: <10 ppb Li and δ^7Li$=0$ to $+8$‰.

Multiple spot analyses of δ^7Li, and scanning ion images of Li composition in Jack Hills zircons reveal that Li concentration and the δ^7Li value correlate with the pattern of magmatic growth-zoning seen in CL images. Correlations of Li concentration with REE, Y, and P concentrations are consistent with both xenotime and interstitial substitution mechanisms, and suggesting that Li^{+1} is important to

charge balance REEs^{+3} in the zircon structure. Concentric zoning with absence of Li enrichment or low δ^7Li values in detrital igneous cores of granulite and amphibolite facies Adirondack zircons also suggests that Li diffusion in zircon is slow. These results are not consistent with sub-solidus alteration, and suggest that zircons preserve primary igneous Li compositions and information constraining the origin of their parent magmas.

The much higher Li concentration in Jack Hills zircons compared to those of zircons from mantle-derived magmas suggests that the Jack Hills zircons crystallized in evolved magmas or magmas contaminated with surface material. The highly variable δ^7Li in Jack Hills zircons can be explained as the result of aqueous alteration at the surface of the Earth. Extremely low δ^7Li observed in zircons as old as ∼4300 Ma requires a low δ^7Li parental magma, implying the magmatic recycling of weathered crust. Thus, Li compositions of Jack Hills zircons support the existence of chemically differentiated and extensive, weathered crust by at least 4300 Ma.

Appendix A. Supplementary data

Supplementary data associated with this article can be found, in the online version, at doi:10.1016/j.epsl.2008.05.032.

References

Beck, P., Chaussidon, M., Barrat, J.A., Gillet, P.H., Bohn, M., 2006. Diffusion induced Li isotopic fractionation during the cooling of magmatic rocks: the case of pyroxene phenocrysts from nakhlite meteorites. Geochim. Cosmochim. Acta 70, 4813–4825.

Benton, L.D., Ryan, G.J., Sanov, I.P., 2004. Lithium abundance and isotope systematics of forearc serpentinite, Conical Seamount, Mariana forearc: insights into the mechanics of slab-mantle exchange during subduction. Geochem. Geophys. Geosyst. 5. doi:10.1029/2004GC000708.

Black, L.P., Kamo, S.L., Allen, C.M., Aleinikoff, J.N., Davis, D.W., Korsch, R.J., Foudoulis, C., 2003. TEMORA 1: a new zircon standard for Phanerozoic U–Pb geochronology. Chem. Geol. 200, 155–170.

Black, L.P., Kamo, S.L., Allen, C.M., Davis, D.W., Aleinikoff, J.N., Valley, J.W., Mundil, R., Campbell, I.H., Korsch, R.J., Williams, I.S., Foudoulis, C., 2004. Improved ^{206}Pb/^{238}U microprobe geochronology by the monitoring of a trace-element-related matrix effect; SHRIMP, ID-TIMS, ELA-ICP-MS and oxygen isotope documentation for a series of zircon standards. Chem. Geol. 205, 115–140.

Bouman, C., Elliott, T., Vroon, P.Z., 2004. Lithium inputs to subduction zone. Chem. Geol. 212, 59–79.

Bryant, C.J., Chappell, B.W., Bennett, V.C., McCulloch, M.T., 2004. Lithium isotopic compositions of the New England Batholith: correlations with inferred source rock compositions. Trans. R. Soc. Edinb. Earth Sci. 95, 199–214.

Cavosie, A.J., 2005. Geochemistry of >3900 Ma Detrital Zircons from Jack Hills, Western Australia. Ph. D. thesis. University of Wisconsin-Madison.

Cavosie, A.J., Valley, J.W., Wilde, S.A., E.I.M.F., 2005a. Magmatic δ^{18}O in 4400–3900 Ma detrital zircons: a record of the alteration and recycling of crust in the Early Archean. Earth Planet. Sci. Lett. 235, 663–681.

Cavosie, A.J., Kita, N.T., Valley, J.W., 2005b. Magmatic δ^{18}O in zircons from gabbros and serpentinized peridotite in the Mid-Atlantic Ridge (ODP Leg 153). Eos Trans. AGU 86 (52), F1887.

Cavosie, A.J., Wilde, S.A., Liu, D., Weiblen, P.W., Valley, J.W., 2004. Internal zoning and U–Th–Pb chemistry of Jack Hills detrital zircons: a mineral record of early Archean to Mesoproterozoic (4348–1576 Ma) magmatism. Precambrian Res. 135, 251–279.

Cavosie, A.J., Valley, J.W., Wilde, S.A., E.I.M.F., 2006. Correlated microanalysis of zircon: trace element, δ^{18}O, and U–Th–Pb isotopic constraints on the igneous origin of complex >3900 Ma detrital grains. Geochim. Cosmochim. Acta 70, 5601–5616.

Cavosie, A.J., Valley, J.W., Wilde, S.A., 2007. The oldest terrestrial mineral record: a review of 4400 to 3900 Ma detrital zircons from Jack Hills, Western Australia. In: Van Kranendonk, M.J., Smithies, R.H., Bennett, V. (Eds.), Earth's Oldest Rocks, Developments in Precambrian Geology, 15. Elsevier, Amsterdam, pp. 91–111.

Chan, L.H., Frey, F.A., 2003. Lithium isotope geochemistry of the Hawaiian plume: results from the Hawaii Scientific Drilling Project and Koolau Volcano. Geochem. Geophys. Geosyst. 4. doi:10.1029/2002GC000365.

Chan, L.H., Edmond, J.M., Thompson, G., Gillis, K., 1992. Lithium isotopic composition of submarine basalts: implications for the lithium cycle in the oceans. Earth Planet. Sci. Lett. 108, 151–160.

Chan, L.H., Alt, J.C., Teagle, D.A.H., 2002a. Lithium and lithium isotope profiles through the upper oceanic crust: a study of seawater-basalt exchange at ODP Sites 504A and 896A. Earth Planet. Sci. Lett. 201, 187–201.

Chan, L.H., Leeman, W.P., You, C.-F., 2002b. Lithium isotopic composition of Central American volcanic arc lavas: implications for modification of subarc mantle by slab-derived fluids: correction. Chem. Geol. 182, 293–300.

Chan, L.H., Leeman, W.P., Plank, T., 2006. Lithium isotopic composition of marine sediments. Geochem. Geophys. Geosyst. 7. doi:10.1029/2005GC001202.

Cherniak, D.J., Watson, E.B., 2003. Diffusion in zircon. In: Hanchar, J.M., Hoskin, P.W.O. (Eds.), Zircon. Rev. in Mineral. Geochem., 53, pp. 113–143.

Cherniak, D.J., Hanchar, J.M., Watson, E.B., 1997. Rare-earth diffusion in zircon. Chem. Geol. 134, 289–301.

Clechenko, C.C., Valley, J.W., 2003. Oscillatory zoning in garnet from the Willsboro Wollastonite Skarn, Adirondack Mts, New York: a record of shallow hydrothermal processes preserved in a granulite facies terrane. J. Meta. Geol. 21, 771–784.

Coogan, L.A., Kasemann, S.A., Chakraborty, S., 2005. Rates of hydrothermal cooling of new oceanic upper crust derived from lithium-geospeedometry. Earth Planet. Sci. Lett. 240, 415–424.

Dohmen, R., Kasemann, S., Coogan, L., Chakraborty, S., 2007. Li Diffusion in Olivine. EOS Trans. Am. Geophy. Un. Abstract #MR13C-1396.

Elliot, T., Thomas, A., Jeffcoate, A., Niu, Y., 2006. Lithium isotope evidence for subduction-enriched mantle in the source of mid-ocean-ridge basalts. Nature 443, 565–568.

Finch, R.J., Hanchar, J.M., Hoskin, P.W.O., Burns, P.C., 2001. Rare-earth elements in synthetic zircon: Part 2. A single-crystal X-ray study of xenotime substitution. Am. Mineral. 86, 681–689.

Grimes, C.B., John, B.E., Kelemen, P.B., Mazdab, F.K., Wooden, J.L., Cheadle, M.J., Hanghoj, K., Schwartz, J.J., 2007. Trace element chemistry of zircons from oceanic crust: a method for distinguishing detrital zircon provenance. Geology 35, 643–646.

Halama, R., McDonough, W.F., Rudnick, R.L., Keller, J., Klaudius, J., 2007. The Li isotopic composition of Oldoinyo Lengai: nature of the mantle sources and lack of isotopic fractionation during carbonatite petrogenesis. Earth Planet. Sci. Lett. 254, 77–89.

Halama, R., McDonough, W.F., Rudnick, R.L., Bell, K., 2008. Tracking the lithium isotopic evolution of the mantle using carbonates. Earth Planet. Sci. Lett. 265, 726–742.

Hanchar, J.M., Finch, R.J., Hoskin, P.W.O., Watson, E.B., Cherniak, D.J., Mariano, A.N., 2001. Rare earth elements in synthetic zircon: Part 1. Synthesis, and rare earth element and phosphorus doping. Am. Mineral. 86, 667–680.

Heumann, M.J., Bickford, M.E., Hill, B.M., McLelland, J.M., Selleck, B.W., Jercinovic, M.J., 2006. Timing of anatexis in metapelites from the Adirondack lowlands and southern highlands: a manifestation of the Shawinigan orogeny and subsequent anorthosite–mangerite–charnockite–granite magmatism. GSA Bulletin 118, 1283–1298.

Hoskin, P.W.O., 2005. Trace-element composition of hydrothermal zircon and the alteration of Hadean zircon from the Jack Hills, Australia. Geochim. Cosmochim. Acta. 69, 637–648.

Hoskin, P.W.O., Schaltegger, U., 2003. The composition of zircon and igneous and metamorphic petrogenesis. In: Hanchar, J.M., Hoskin, P.W.O. (Eds.), Zircon. Rev. in Mineral. Geochem., 53. The Mineralogical Society of America, Washington DC, pp. 27–62.

Huh, Y., Chan, L.H., Edmond, J.M., 2001. Lithium isotopes as a probe of weathering processes: Orinoco River. Earth Planet. Sci. Lett. 194, 189–199.

Jeffcoate, A.B., Elliott, T., Kasemann, S.A., Ionov, D., Cooper, K., Brooker, R., 2007. Li isotope fractionation in peridotites and mafic melts. Geochim. Cosmochim. Acta 71, 202–218.

Kasemann, S.A., Jeffcoate, A.B., Elliott, T., 2005. Lithium isotopic composition of basalt glass reference material. Anal. Chem. 77, 5251–5257.

Kasting, J.F., 1993. Earth's early atmosphere. Science 259 , 920–926.

Kisakürek, B., Widdowson, M., James, R.H., 2004. Behaviour of Li isotopes during continental weathering: the Bidar laterite profile, India. Chem. Geol. 212, 27–44.

Kitchen, N.E., Valley, J.W., 1995. Carbon isotope thermometry in marbles of the Adirondack Mountains, New York. J. Metamorph. Geol. 13, 577–594.

Kobayashi, K., Tanaka, R., Moriguti, T., Shimizu, K., Nakamura, E., 2004. Lithium, boron, and lead isotope systematics of glass inclusions in olivines from Hawaiian lavas: evidence for recycled components in the Hawaiian plume. Chem. Geol. 212, 143–161.

Lundstrom, C.C., Chaussidon, M., Hsui, A.T., Kelemen, P., Zimmerman, M., 2005. Observations of Li isotopic variations in the trinity ophiolite: evidence for isotopic fractionation during diffusion during mantle melting. Geochim. Cosmochim. Acta 69, 735–751.

Magna, T., Wiechert, U., Grove, T.L., Halliday, A.N., 2006a. Lithium isotope fractionation in the southern Cascadia subduction zone. Earth Planet. Sci. Lett. 250, 428–443.

Magna, T., Wiechert, U., Halliday, A.N., 2006b. New constraints on the lithium isotope compositions of the Moon and terrestrial planets. Earth Planet. Sci. Lett. 243, 336–353.

Marks, M.A.W., Rudnick, R.L., McCammon, C., Vennemann, T., Markl, G., 2007. Arrested kinetic Li isotope fractionation at the margin of the Ilímaussaq complex, South Greenland: evidence for open-system processes during final cooling of peralkaline igneous rocks. Chem. Geol. 346, 207–230.

McLelland, J.M., Bickford, M.E., Hill, B.M., Clechenko, C.C., Valley, J.W., Hamilton, M.A., 2004. Direct dating of Adirondack massif anorthosite by U–Pb SHRIMP analysis of igneous zircon: implications for AMCG complexes. GSA Bulletin 116, 1299–1317.

Moriguti, T., Nakamura, E., 1998. Across-arc variation of Li isotopes in lavas and implications for crust/mantle recycling at subduction zones. Earth Planet. Sci. Lett. 163, 167–174.

Nemchin, A.A., Pidgeon, R.T., Whitehouse, M.J., 2006. Re-evaluation of the origin and evolution of >4.2 Ga zircons from the Jack Hills metasedimentary rocks. Earth Planet. Sci. Lett. 244, 218–233.

Nishio, Y., Nakai, S., Ishii, T., Sano, Y., 2007. Isotope systematics of Li, Sr, Nd, and volatiles in Indian Ocean MORBs of the Rodriguez Triple Junction: constraints on the origin of the DUPAL anomaly. Geochim. Cosmochim. Acta, 71, 745–759.

Page, F.Z., Fu, B., Kita, N.T., Fournelle, J., Spicuzza, M.J., Schulze, D.J., Viljoen, V., Basei, M.A.S., Valley, J.W., 2007a. Zircons from kimberlites: new insights from oxygen isotopes, trace elements, and Ti in zircon thermometry. Geochim. Cosmochim. Acta 71, 3887–3903.

Page, F.Z., Ushikubo, T., Kita, N.T., Riciputi, L.R., Valley, J.W., 2007b. High-precision oxygen isotope analysis of pictogram samples reveals 2 μm gradients and slow diffusion in zircon. Am. Mineral. 92, 1772–1775.

Parkinson, I.J., Hammond, S.J., James, R.H., Roger, N.W., 2007. High-temperature lithium isotope fractionation: insights from lithium isotope diffusion in magmatic systems. Earth Planet. Sci. Lett. 257, 609–621.

Pearce, N.J.G., Perkins, W.T., Westgate, J.A., Gorton, M.P., Jackson, S.E., Neal, C.R., Chenery, S.P.A., 1996. Compilation of new and published major and trace element data for NIST SRM 610 and NIST SRM 612 glass reference materials. Geostandards Newslett. 21, 115–145.

Peck, W.H., Valley, J.W., Graham, C.M., 2003. Slow oxygen diffusion rates in igneous zircons from metamorphic rocks. Am. Mineral. 88, 1003–1014.

Richter, F.M., Davis, A.M., DePaolo, D.J., Watson, E.B., 2003. Isotope fractionation by chemical diffusion between molten basalt and rhyolite. Geochim. Cosmochim. Acta 67, 3905–3923.

Rudnick, R.L., Ionov, D.A., 2007. Lithium elemental and isotopic disequilibrium in minerals from peridotite xenoliths from far-east Russia: product of recent melt/fluid- rock reaction. Earth Planet. Sci. Lett. 256, 278–293.

Rudnick, R.L., Tomascak, P.B., Njo, H.B., Gardner, L.R., 2004. Extreme lithium isotopic fractionation during continental weathering revealed in saprolites from South Carolina. Chem. Geol. 212, 45–57.

Ryan, J.G., Kyle, P.R., 2004. Lithium abundance and lithium isotope variations in mantle sources: insights from intraplate volcanic rocks from Ross Island and Marie Byrd Land (Antarctica) and other oceanic islands. Chem. Geol. 212, 125–142.

Seitz, H.-M., Brey, G.P., Lahaye, Y., Durali, S., Weyer, S., 2004. Lithium isotopic signatures of peridotite xenoliths and isotopic fractionation at high temperature between olivine and pyroxenes. Chem. Geol. 212, 163–177.

Seitz, H.-M., Brey, G.P., Zipfel, J., Ott, U., Weyer, S., Durali, S., Weinbruch, S., 2007. Lithium isotope composition of ordinary and carbonaceous chondrites, and differentiated planetary bodies: bulk solar system and solar reservoir. Earth Planet. Sci. Lett. 260, 582–596.

Spandler, C., O'Neill, H.STC., 2006. Trace-Element Diffusion Coefficients in Olivine. EOS Trans. Am. Geophy. Un. Abstract #V53E-02.

Shannon, R.D., 1976. Revised effective ionic radii and systematic studies of interatomic distances in halides and chalcogenides. Acta. Cryst. A32, 751–767.

Teng, F.-Z., McDonough, W.F., Rudnick, R.L., Dalpé, C., Tomascak, P.B., Chappell, B.W., Gao, S., 2004. Lithium isotopic composition and concentration of the upper continental crust. Geochim. Cosmochim. Acta 68, 4167–4178.

Teng, F.-Z., McDonough, W.F., Rudnick, R.L., Walker, R.J., 2006b. Diffusion-driven extreme lithium isotopic fractionation in country rocks of the Tin Mountain pegmatite. Earth Planet. Sci. Lett. 243, 701–710.

Teng, F.-Z., McDonough, W.F., Rudnick, R.L., Walker, J., Sirbescu, M.-L.C., 2006a. Lithium isotopic systematics of granites and pegmatites from the Black Hills, South Dakota. Am. Mineral. 91, 1488–1498.

Teng, F.-Z., McDonough, W.F., Rudnick, R.L., Wing, B.A., 2007. Limited lithium isotopic fractionation during progressive metamorphic dehydration in metapelites: a case study from the Onawa contact aureole, Maine. Chem. Geol. 239, 1–12.

Tomascak, P.B., 2004. Developments in the understanding and application of lithium isotopes in the early and planetary science. In: Johnson, C.M., Beard, B.L., Albarède, F. (Eds.), Geochemistry of Non-Traditional Stable Isotopes. Rev. in Mineral. Geochem, 55. Mineralogical Society of America, Washington DC, pp. 153–195.

Tomascak, P.B., Tera, F., Helz, R.T., Walker, R.J., 1999. The absence of lithium isotope fractionation during basalt differentiation: new measurements by multicollector sector ICP-MS. Geochim. Cosmochim. Acta 63, 907–910.

Tomascak, P.B., Ryan, J.G., Defant, M.J., 2000. Lithium isotope evidence for light element decoupling in the Panama subarc mantle. Geology 28, 507–510.

Tomascak, P.B., Langmuir, C.H., le Roux, P.J., 2008. Lithium isotopes in global mid-ocean ridge basalts. Geochim. Cosmochim. Acta 72, 1626–1637.

Valley, J.W., Bohlen, S.R., Essene, E.J., Lamb, W., 1990. Metamorphism in the Adirondacks: II. The role of fluids. J. Petrol. 31, 555–596.

Wiedenbeck, M., Hanchar, J.M., Peck, W.H., Sylvester, P., Valley, J., Whitehouse, M., Kronz, A., Morishita, Y., Nasdala, L., Feibig, J., Franchi, I., Girard, J.-P., Greenwood, R.C., Hinton, R., Kita, N., Mason, P.R.D., Norman, M., Ogasawara, S.M., Piccoli, P.M., Rhede, D., Satoh, H., Schulz-Dobrick, B., Skår, Ø., Spicuzza, M.J., Terada, K., Tindle, A., Togashi, S., Vennemann, T., Xie, Q., Zheng, Y.-F., 2004. Further characterization of the 91500 zircon crystal. Geostandards and Geoanalytical Research 28, 9–39.

Wunder, B., Meixner, A., Romer, R.L., 2006. Temperature-dependent isotopic fractionation of lithium between clinopyroxene and high-pressure hydrous fluids. Contrib. Mineral. Petrol. 151, 112–120.